BIOMOLECULES & THERAPEUTICS

Original Article
Biomol Ther 32(5), 556-567 (2024)

Investigating the Immune-Stimulating Potential of β-Glucan from *Aureobasidium pullulans* in Cancer Immunotherapy

Jae-Hyeon Jeong[1,2,3,†], Dae-Joon Kim[1,2,3,†], Seong-Jin Hong[4,5,†], Jae-Hee Ahn[1,3], Dong-Ju Lee[1,2,3], Ah-Ra Jang[6], Sungyun Kim[1,2], Hyun-Jong Cho[1,2], Jae-Young Lee[6], Jong-Hwan Park[6,7], Young-Min Kim[4,5,*] and Hyun-Jeong Ko[1,2,3,6,*]

[1]*Department of Pharmacy, Kangwon National University, Chuncheon 24341,*
[2]*KNU Researcher training program for Innovative Drug Development Research Team for Intractable Diseases (BK21 plus), Kangwon National University, Chuncheon 24341,*
[3]*Global/Gangwon Innovative Biologics-Regional Leading Research Center (GIB-RLRC), Kangwon National University, Chuncheon 24341,*
[4]*Institute of Agricultural Science and Technology, Chonnam National University, Gwangju 61186,*
[5]*Department of Integrative Food, Bioscience and Biotechnology, Chonnam National University, Gwangju 61186,*
[6]*Nodcure, Inc., Gwangju 61186,*
[7]*Laboratory Animal Medicine, Animal Medical Institute, College of Veterinary Medicine, Chonnam National University, Gwangju 61186, Republic of Korea*

Abstract

β-glucan, a polysaccharide found in various sources, exhibits unique physicochemical properties, yet its high polymerization limits its clinical applications because of its solubility. Addressing this limitation, we introduce PPTEE-glycan, a highly purified soluble β-1,3/1,6-glucan derived from *Aureobasidium pullulans*. The refined PPTEE-glycan demonstrated robust immune stimulation *in vitro*, activated dendritic cells, and enhanced co-stimulatory markers, cytokines, and cross-presentation. Formulated as a PPTEE + microemulsion (ME), it elevated immune responses *in vivo*, promoting antigen-specific antibodies and CD8+ T cell proliferation. Intratumoral administration of PPTEE + ME in tumor-bearing mice induced notable tumor regression, which was linked to the activation of immunosuppressive cells. This study highlights the potential of high-purity *Aureobasidium pullulans*-derived β-glucan, particularly PPTEE, as promising immune adjuvants, offering novel avenues for advancing cancer immunotherapy.

Key Words: β-glucan, Vaccine, Antigen-presenting cell, Myeloid-derived suppressive cell, Formulation, Cancer

INTRODUCTION

Cancer therapy has undergone notable evolution, progressing from conventional chemotherapy to contemporary immunotherapy strategies (Schirrmacher, 2019). Although immunotherapy has revolutionized cancer treatment, offering superior anti-cancer effects with minimal side effects compared to traditional approaches such as chemotherapy and radiotherapy (Tan *et al*., 2020), challenges persist, particularly in achieving consistent response rates across various cancer types (Schoenfeld and Hellmann, 2020). To address these challenges, combination therapies co-treating chemotherapy and immunotherapy with adjuvants have emerged as promising avenues (Bayat Mokhtari *et al*., 2017; Lin *et al*., 2022). Adjuvants play a pivotal role in enhancing vaccine effectiveness by amplifying the immune response (Pulendran *et al*., 2021). Innovations in adjuvant formulations such as emulsions, liposomes, and nanoparticles combined with pattern recognition receptor (PRR) ligands have contributed significantly to augmenting immune reactions to antigens (Kawai and Akira, 2010; Reed *et al*., 2013). The adoption of adjuvants as immune stimulators in cancer immunotherapy is based on their ability to enhance anti-tumor immune responses, inhibit tumor growth, and eliminate tumor cells.

Open Access **https://doi.org/10.4062/biomolther.2024.047**

Received Mar 20, 2024 **Revised** May 24, 2024 **Accepted** Jun 10, 2024
Published Online Aug 2, 2024

***Corresponding Authors**
E-mail: hjko@kangwon.ac.kr (Ko HJ), u9897854@jnu.ac.kr (Kim YM)
Tel: +82-33-250-6923 (Ko HJ), +82-62-530-2142 (Kim YM)
Fax: +82-62-530-2169 (Kim YM)
[†]The first three authors contributed equally to this work.

Tumor interacts with various immune cells in the tumor microenvironment (TME) to maintain an immunosuppressive milieu (Baghban *et al*., 2020). Overcoming this immunosuppressive environment and effectively attacking tumors requires stimulation of the immune system (Baghban *et al*., 2020). Immune stimulators, including β-glucan, toll-like receptor (TLR) agonists, cytokines, and immune checkpoint inhibitors, play a crucial role in activating immune cells, thereby facilitating the recognition and destruction of tumor cells (Hong *et al*., 2004; Huang *et al*., 2018; Berraondo *et al*., 2019; Toor *et al*., 2020). This study focused on the strategic utilization of diverse immune stimulators, with particular emphasis on β-glucan, in cancer immunotherapy.

β-glucan, particularly mainly derived from *Aureobasidium pullulans*, exhibits distinctive characteristics that position them as one of the promising candidates for immune adjuvants, serving as effective immune stimulators in cancer therapy (Shui *et al*., 2021; Ikewaki *et al*., 2022). The innate immune system has opened a novel avenue for enhancing vaccine efficacy by triggering TLRs in dendritic cells using pathogen-associated molecular patterns (PAMPs), thereby strengthening T cell and B cell responses (Kawai and Akira, 2010). β-glucan exhibits immune-modulating properties by binding to receptors like complement receptor 3 (CR3) or Dectin-1 on innate cells, inducing the production of pro-inflammatory cytokines and altering epigenetic reprogramming of myeloid cells, initiating "Trained immunity." Additionally, β-glucan activates lymphocytes, enhancing humoral immunity (Goodridge *et al*., 2009; Camilli *et al*., 2018; Moorlag *et al*., 2020). These attributes collectively position β-glucan as a robust immune adjuvant. Extensive studies have explored the immunostimulatory effects, macrophage activation, pathogen clearing, and production of proinflammatory cytokines (Lei *et al*., 2015; Vetvicka and Vetvickova, 2015; Albeituni *et al*., 2016; Camilli *et al*., 2018). Their potential medical applications include the treatment of various infections and the alleviation of chemotherapy side effects in cancer patients with cancer.

In this study, we obtained a soluble β-1,3/1,6-glucan (PPTEE) with high purity from *Aureobasidium pullulans* and explored its potential as a vaccine adjuvant and anti-cancer immunotherapeutic.

MATERIALS AND METHODS

Animal and immunization

All animal experiments were conducted with the approval of the Institutional Animal Care and Use Committee of Kangwon National University (IACUC No. KW-221102-2). Female C57BL/6 mice, aged 5 weeks, were purchased from Koatech Co. Ltd (Pyeongtaek, Korea) and housed in the Specific Pathogen-Free facility at the Laboratory Animal Research Center of Kangwon National University. The mice received intramuscular immunizations every 2 weeks for a total of 6 weeks. Each mouse groups were administered 10 μg of Ovalbumin (OVA, Sigma Aldrich, St. Louis, MO, USA) alone, OVA+microemulsion (ME) and OVA+ME-containing 100 μg of PPTEE-glucan, as an adjuvant, for immunization.

Sample preparation and purification

A seed culture of *Aureobasidium pullulans* KCTC 6459 was initiated by inoculating 200 mL of potato dextrose agar (PDA) medium and then cultured at 25°C with agitation at 200 rpm for 1 day. The main culture was established by transferring the seed culture to 2,000 mL of PDA supplemented with 50% (w/v) glucose at 30°C with agitation at 200 rpm for 4 days to facilitate optimal growth and metabolite production. After the incubation period, the culture broth underwent centrifugation at 8,000×g for 5 min to separate the microbial biomass from the supernatant. The supernatant was subsequently vacuum-filtered through Hyundai Micro No. 20 filter paper (5-8 μm, Seoul, Korea) to eliminate any remaining cell debris.

Treatment with pullulanase (Promozyme D2, Daejongzymes, Seoul, Korea) was carried out by incubating the supernatant at 30°C with agitation at 200 rpm for 24 h to enzymatically break down pullulan. Following this, the supernatant was subjected to protease treatment (Protamex, Daejongzymes) at 50°C for 24 h. To precipitate the proteins, 100% (v/v) trichloroacetic acid (TCA) was added to the treated supernatant to achieve a final concentration of 6% (v/v) TCA, which was then cooled at 4°C overnight. The TCA-treated mixture was centrifuged at 8,000×g for 20 min to pellet the precipitated polysaccharides. The supernatant was carefully decanted, leaving the precipitate behind.

The precipitate was resuspended in 2.5 volumes of ice-cold ethanol and stored at –20°C overnight to further facilitate polysaccharide precipitation. After incubation, the mixture underwent another round of centrifugation at 8,000×g for 20 min to collect the polysaccharide precipitate. The collected precipitate was reconstituted with distilled water and then subjected to a second round of ethanol precipitation by adding 2.5 volumes of ice-cold ethanol and incubating at –20°C overnight. Subsequently, the mixture was centrifuged at 8,000×g for 20 min to pellet the polysaccharides, which were washed with distilled water to remove any residual ethanol. Finally, the washed polysaccharide precipitate was lyophilized to obtain dry PPTEE-glucan samples for further analysis.

Quantification of β-glucan levels using enzymatic analysis

Following the manufacturer's protocol, we quantified β-glucan levels using the Megazyme yeast β-glucan enzymatic kit (Megazyme, Bray, Ireland). The samples were dissolved in sodium hydroxide. After pH adjustment, the glucan was converted into glucose by β-glucanases, β-glucosidases, and chitinases, and then quantified using the GOPOD reagent. The entire process was conducted in accordance with the manufacturer's guidelines, and each sample underwent the assay three times.

Determination of total sugar content in β-glucan

The total sugar content of β-glucan was determined using the phenol-sulfuric acid method (DuBois *et al*., 1956). Specifically, 500 μL of the sample and 500 μL of 5% (v/v) phenol were combined in a glass test tube, followed by the addition of 2.5 mL of sulfuric acid and thorough mixing. The mixture was then incubated at 80°C for 20 min, and the absorbance was measured at 490 nm. To quantify the total sugar content, a standard calibration curve was established with glucose as the standard substance, and the total sugar content was calculated based on this curve.

Determination of total protein content in β-glucan

The total protein content in β-glucan was determined using the Bradford method. In detail, 15 μL of the sample solution

and 750 μL of the Bradford reagent were combined in a tube and incubated at room temperature for 5 min. Subsequently, the absorbance was measured at 595 nm. To quantify the total protein content, a standard calibration curve was established with Bovine Serum Albumin as the standard substance, and the total protein content was calculated based on this curve. The total protein content (%) of β-glucan was then calculated accordingly.

Analysis of molecular weight distribution of β-glucan

The molecular weight distribution of the β-glucan was analyzed using high-performance size-exclusion chromatography (HPSEC) with two series-connected Shodex columns, specifically KS-804 and KS-802 (Showa Denko, Tokyo, Japan). The samples were dissolved in a dimethyl sulfoxide/water mixture (90:10; v/v). The column was maintained at a constant temperature of 70°C, and the mobile phase (water) was delivered at a flow rate of 0.8 mL/min. The distribution was compared with pullulan standards (Shodex P-82, Showa Denko). These standards were prepared by allowing a 0.05% (w/v) aqueous solution to stand at 25°C for 24 h, resulting in complete particle swelling. The dispersion was stirred until all particles dissolved. Prior to use, the solution was filtered through a 0.45 μm filter.

In vivo tumor model with PPTEE-glucan and QS-21 administration

A female C57BL/6 mouse was subcutaneously injected with MC38 colon cancer cells (1×10^6). The mouse received intratumoral injections of QS-21 (1 μg) or a combination of PPTEE-glucan (100 μg) with ME, each in 50 μL, every 3 days starting from day 7 post-tumor inoculation until the conclusion of the experiment. Tumor size was monitored every other day until reaching a volume of 1,500 mm^3 (calculated as length×width×2/2). Subsequently, the mice were euthanized to extract the tumors.

Isolation of tumor-infiltrating mononuclear cells

The tumor tissue was homogenized in a C-tube (Miltenyi Biotec, Bergisch Gladbach, Germany) containing 5 mL of digestion buffer [RPMI-1640 (Corning, NY, USA) with 2% Bovine serum (Gibco, Waltham, MA, USA), 10 mM HEPES (Welgene, Gyeongsan, Korea), 1% Penicillin/Streptomycin (Welgene), 400 U/mL Collagenase IV (Worthington Biochemical, Lakewood, NJ, USA), and 0.1 mg/mL DNase I (Roche Diagnostics, Basel, Switzerland)] using GentleMACS (Miltenyi Biotec). The digestion buffer was incubated in a shaking incubator at 200 rpm, 37°C for 45 min. The digested tumor tissues were filtered through a 100 μm pore size strainer, and 10 mL of PBS (Corning) was added before centrifugation at 1,400 rpm for 3 min at 4°C. After removing the supernatant, the pellet was suspended with 40% Percoll (Cytiva, Marlborough, MA, USA) and layered on 70% Percoll. Density gradient separation was carried out at 2,000 rpm for 20 min at room temperature without interruption. The white ring between the 40/70 Percoll layers was collected, washed with 10 mL PBS at 1,400 rpm for 3 min at 4°C, and the cell pellet was suspended in PBS for further analysis.

Flow cytometry analysis of tumor-infiltrating mononuclear cells

The extracted tumor cells were first incubated with PBS containing αCD16/CD32 (2.4G2) at room temperature for 10 min to block Fc receptors. Subsequently, the cells were incubated with a diverse combination of antibodies in PBS, including APC-Cy7-Ly6C (HK1.4), PE-PD-L1 (10F.9G2), PE-Cy7-Ly6G (1A8), PerCP-Cy5.5-CD45 (30-F11), BV421-CD11b (M1/70), and Fixable Viability Dye NIR (Invitrogen, Waltham, MA, USA), in the dark for 30 min at 4°C for cell surface staining. The tumor cells were then centrifuged at 1,400 rpm for 3 min at 4°C for washing. After removing the supernatant, the pellet was suspended in PBS. All fluorochrome-conjugated antibodies were obtained from BioLegend (San Diego, CA, USA). The stained tumor cells were analyzed using FACSVerse flow cytometry (BD Bioscience, Franklin Lakes, NJ, USA) and FlowJo Version 10.8.1 software (BD Bioscience).

Differentiation of BM-derived cells preparation and stimulation

The tibia and femur of a mouse were extracted to flush out bone marrow (BM) cells with PBS, followed by the removal of red blood cells (RBCs) using an RBC lysis buffer (Invitrogen) and filtration through a 100 μm pore size strainer. The isolated BM cells were cultured in a growth medium with GM-CSF (20 ng/mL) and IL-4 (20 ng/mL) for 6 days at 37°C with 5% CO_2 to differentiate into dendritic cells (DC). Subsequently, the BM-derived DC (BMDC) were stimulated with PPTEE-glucan (10 μg/mL), QS-21 (1 μg/mL), and OVA (10 μg/mL) for 24 h at 37°C with 5% CO_2 before further analysis. Similarly, the tibia and femur of a mouse were used to extract BM cells, which were then processed to remove RBCs and cultured in a growth medium with GM-CSF (20 ng/mL) and IL-6 (10 ng/mL) for 5 days at 37°C with 5% CO_2 to differentiate into myeloid-derived suppressive cells (MDSC). The BM-derived MDSC were stimulated with PPTEE-glucan or QS-21 for 24 h at 37°C with 5% CO_2 before subsequent analysis.

Analysis of co-stimulatory markers on bone marrow-derived dendritic cells

The stimulated BMDC were incubated with PBS containing αCD16/CD32 (2.4G2) at room temperature for 10 min to block Fc receptors. Subsequently, the cells were incubated with a diverse combination of antibodies, including PE-CD80 (16-10A1), APC-CD86 (GL-1), FITC-CD11c (N418), PE-Cy7-CD40 (3/23), PerCP-Cy5.5-H2-K^b (AF6-88.5), Pacific Blue-I-A/I-E (M5/114.15.2), and Fixable Viability Dye NIR (Invitrogen), in the dark for 30 min at 4°C for cell surface staining. The BMDC were then centrifuged at 1,400 rpm for 3 min at 4°C for washing. After removing the supernatant, the pellet was suspended in PBS. All fluorochrome-conjugated antibodies were purchased from BioLegend. The stained BMDC were analyzed using FACSVerse flow cytometry (BD Bioscience) and FlowJo Version 10.8.1 software (BD Bioscience).

Cross-presentation analysis of bone marrow-derived dendritic cells

The stimulated BMDC (5×10^4) were seeded into a U-bottom 96-well plate. OT-I mice were sacrificed to extract the spleen and lymph nodes. The spleen and lymph nodes were minced on a 100 μm pore size strainer using a syringe piston in PBS. The PBS was collected into a 15 mL tube and centrifuged at 1,400 rpm for 3 min at 4°C. After removing the supernatant, the pellet was suspended with RBC lysis buffer (Invitrogen) to remove red blood cells. The sample was centrifuged at 1,400

rpm for 3 min at 4°C. The supernatant was removed, and the pellet was suspended in PBS. The PBS was filtered through a 100 μm pore size strainer. $CD8^+$T cells in the sample were isolated using the $CD8^+$T cell isolation kit (Miltenyi Biotec) and then stained with CellTrace Violet (CTV, Invitrogen) following the manufacturer's instructions. The $CD8^+$T cells were seeded into wells containing BMDC and co-cultured in growth medium for 2 days at 37°C with 5% CO_2. The cells were collected, incubated with PBS containing αCD16/CD32 (2.4G2) at room temperature for 10 min to block Fc receptors. Subsequently, the cells were incubated with PBS containing a diverse combination of antibodies, including APC-CD8 (53-6.7), PE-CD45.1 (A20), and Fixable Viability Dye NIR (Invitrogen), in the dark for 30 min at 4°C for cell surface staining. The cells were then centrifuged at 1,400 rpm for 3 min at 4°C for washing. After removing the supernatant, the pellet was suspended in PBS. All fluorochrome-conjugated antibodies were purchased from BioLegend. The stained cells were analyzed using FACSVerse flow cytometry (BD Bioscience) and FlowJo Version 10.8.1 software (BD Bioscience).

OVA-containing ME+PPTEE preparation and its particle characterization

The emulsion composition, consisting of oil, surfactant, and cosurfactant, was chosen based on our prior research (Lee *et al*., 2016). Labrasol (165 mg, Sigma Aldrich) was combined with Tween 80 (50 mg, Sigma Aldrich), and mineral oil (10 mg, Sigma Aldrich) was then added to the mixture. In the water phase, PPTEE (1.98 mg) was dissolved in distilled water (275 mg). To form the ME+PPTEE, the water phase was mixed with the oil/surfactant mixture. For the OVA-containing ME+PPTEE, a two-fold concentration of the OVA solution (compared to the final OVA concentration in the emulsion) was mixed with the prepared ME+PPTEE at a 1:1 volume ratio. Hydrodynamic size and zeta potential values of ME+PPTEE and OVA+ME+PPTEE formulations were measured by particle size & zeta potential analyzer (ELS-Z1000, Otsuka Electronics, Tokyo, Japan). The morphological shapes of ME+PPTEE and OVA+ME+PPTEE were observed by transmission electron microscopy (TEM) (JEM-2100F; JEOL, Tokyo, Japan). The entrapment efficiency of PPTEE in ME was measured by high-performance liquid chromatography (HPLC) system (LC-20, Shimadzu, Kyoto, Japan). The mobile phase was 100% acetonitrile (ACN). The analysis was done under the isocratic condition with the reverse phase C18 column (Asahipak ODP-50 4E, 250 mm×4.6 mm, 5 μm; Shodex, New York, NY, USA). The flow rate was fixed at 0.5 mL/min.

Spleen cell isolation and splenocyte antigen stimulation

The spleen was minced on a 100 μm pore size strainer using a syringe piston in PBS. The PBS containing the minced spleen was collected in a 15 mL tube and centrifuged at 1,400 rpm for 3 min at 4°C. After removing the supernatant, the cell pellet was suspended in 1 mL of RBC lysis buffer (Invitrogen) and incubated for 1 min at room temperature. Following the addition of 4 mL of PBS, the tube was centrifuged at 1,400 rpm for 3 min at 4°C. After discarding the supernatant, the pellet was resuspended in 10 mL of PBS and filtered through a 100 μm pore size strainer, making the sample ready for further study. Splenocytes from OVA-vaccinated mice (2×10^5) were seeded into a round-bottom 96-well plate containing growth medium with 10 μg of OVA at 37°C with 5% CO_2 for 3 days. The cells were then collected in a 1.5 mL tube, followed by intracellular staining as described above.

Intracellular staining and cytokine analysis using flow cytometry

Harvested cells from the tumor or spleen were stimulated with 200 μL of growth medium, including Cell Stimulation Cocktail plus a protein transport inhibitor (eBioscience, Waltham, MA, USA), for 3 h in a 37°C, 5% CO_2 incubator. The cells were then collected in a 1.5 mL tube and washed with 1 mL of PBS by centrifuging at 1,400 rpm for 3 min at 4°C. Subsequently, the cells were incubated with PBS containing αCD16/CD32 (2.4G2) at room temperature for 10 min to block Fc receptors. The cells were further incubated with a diverse combination of antibodies, including FITC-CD3 (145-2C11), PerCP-Cy5.5-CD4 (GK1.5), PE-Cy7-CD8 (53-6.7), PE-CD45 (30-F11), and Fixable Viability Dye NIR for T cells, and PE-Cy7-CD11b (M1/70), BV510-F4/80 (BM8), FITC-Ly6C (HK1.4), BV421-CD45 (30-F11), and Fixable Viability Dye NIR for MDSC. The cells were incubated in the dark for 30 min at 4°C for cell surface staining. Following this, the cells were treated with IC fixation buffer (eBioscience) for 30 min in the dark at 4°C for cell permeabilization. The fixed cells were washed with 1× permeabilization buffer (eBioscience) using a centrifuge as described in the previous step. For cytokine staining, the cells were incubated with 1× Permeabilization buffer containing APC-IFN-γ (XMG1.2) and APC-TNF-α (MP6-XT22) for T cells and MDSC, respectively, in the dark for 30 min at 4°C. Subsequently, the cells were washed with 1× Permeabilization buffer using a centrifuge as described earlier, and the pellet was suspended in 1× Permeabilization buffer. The stained cells were analyzed using FACSVerse flow cytometry (BD Bioscience) and FlowJo Version 10.8.1 software (BD Bioscience). All fluorochrome-conjugated antibodies were purchased from BioLegend.

Cytokine analysis by ELISA

The supernatant from stimulated BMDC and MDSC was collected in a 1.5 mL tube, then centrifuged at 13,000 rpm for 10 minutes at 4°C. The supernatant was transferred to a new 1.5 mL tube. TNF-α, IL-1β, IL-6, and IL-12p40 were measured using respective ELISA kits (Invitrogen) following the manufacturer's instructions.

Serum ovalbumin-specific antibody detection by ELISA

Immuno 96-well plates (Thermo Fisher Scientific, Waltham, MA, USA) were coated with 10 μg/mL of OVA in 0.05 M carbonate-bicarbonate buffer (pH 9.6, Sigma Aldrich) and incubated overnight at 4°C. The wells were washed three times using PBS containing 0.05% Tween-20 (PBS-T) and then blocked with 1% bovine serum albumin (BSA, MP Biomedicals, Solon, OH, USA) for 1 h at room temperature. After washing the wells with PBS-T, diluted serum samples were added to the wells and incubated overnight at 4°C. Subsequently, the wells were washed three times with PBS-T, and horseradish peroxidase-conjugated goat anti-mouse IgG1, anti-mouse IgG2b, anti-mouse IgG2c, or anti-mouse IgM (Southern Biotech, Birmingham, AL, USA) were added and incubated for 2 h at room temperature. Following five washes with PBS-T, TMB substrate (Surmodics, Eden Prairie, MN, USA) was added to the wells and incubated for 15 min at room temperature. The reaction was stopped by adding 0.5 M HCl. The optical den-

sity (O.D.) of the wells in the plates was measured at 450 nm using a microplate reader (Molecular Devices, San Jose, CA, USA).

In vivo OT-I CD8$^+$T cell proliferation assay

Recipient mice were infused with CTV (Invitrogen)-stained OT-I CD8$^+$T cells (1×10^6) via intravenous injection. The following day, the mice received subcutaneous administration of OVA (10 μg) along with either QS-21 (1 μg) or a combination of PPTEE-glucan (100 μg) with ME. Three days post-OVA injection, the mice were euthanized, and their spleens were harvested for the analysis of proliferated OT-I CD8$^+$T cells using FACSVerse flow cytometry (BD Bioscience) and FlowJo Version 10.8.1 software (BD Bioscience).

TUNEL assay for apoptosis detection in mouse tumor tissue

The mouse tumor tissue was fixed in 4% formaldehyde for 24 h and dehydrated using ethanol in a Tissue Processor (Leica, Wetzlar, Germany). Subsequently, the tissues were embedded in paraffin and sectioned into 5 μm-thick slices. Slides containing these sections were incubated at 60°C for 1 h, deparaffinized using xylene, and rehydrated with graded ethanol. Apoptosis was assessed using a TUNEL assay kit (Thermo Fisher Scientific), following the manufacturer's protocol. The slides were mounted with a mounting solution containing 4',6-diamidino-2-phenylindole (DAPI, BioLegend) for confocal microscopy.

Statistical analysis

Statistical analyses were conducted using GraphPad Prism version 9 (GraphPad Software LLC, San Diego, CA, USA). The unpaired t-test was used to assess the differences between tow groups. The comparisons among multiple groups utilized Dunnett's test and one-way analysis of variance (ANOVA). Furthermore, for comparisons involving groups with continuous values, two-way ANOVA was employed. The threshold for statistical significance was set at $p<0.05$, with 95% confidence intervals estimated for all analyses.

RESULTS

PPTEE-glucan production and purification

Aureobasidium pullulans KCTC 6459 was cultured in 2 L of PDA supplemented with 50% (w/v) glucose at 30°C with agitation at 200 rpm for 5 days. We optimized the following four separate purification processes, including PE, PPE, PPTE, and PPTEE, to obtain the high purity of β-glucan (Fig. 1A). As the refinement conditions intensified, a corresponding increase was observed in both the β-glucan content and total sugar content. The PPTEE condition recorded the highest β-glucan content at 3.42 ± 0.42 g/L and the peak total sugar content at 98.84 ± 0.45% (Fig. 1B, 1C). This indicated the effectiveness of the purification process and suggesting that PPTEE was primarily composed of PPTEE-glucan (PPTEE). Conversely, the total protein content exhibited a decreasing trend with the intensification of the purification conditions, reaching a significantly lower concentration under PPTEE conditions (Fig. 1D). While evaluating the molecular weight distribution at each purification step, we observed that a more diverse range of molecular sizes was present under simpler

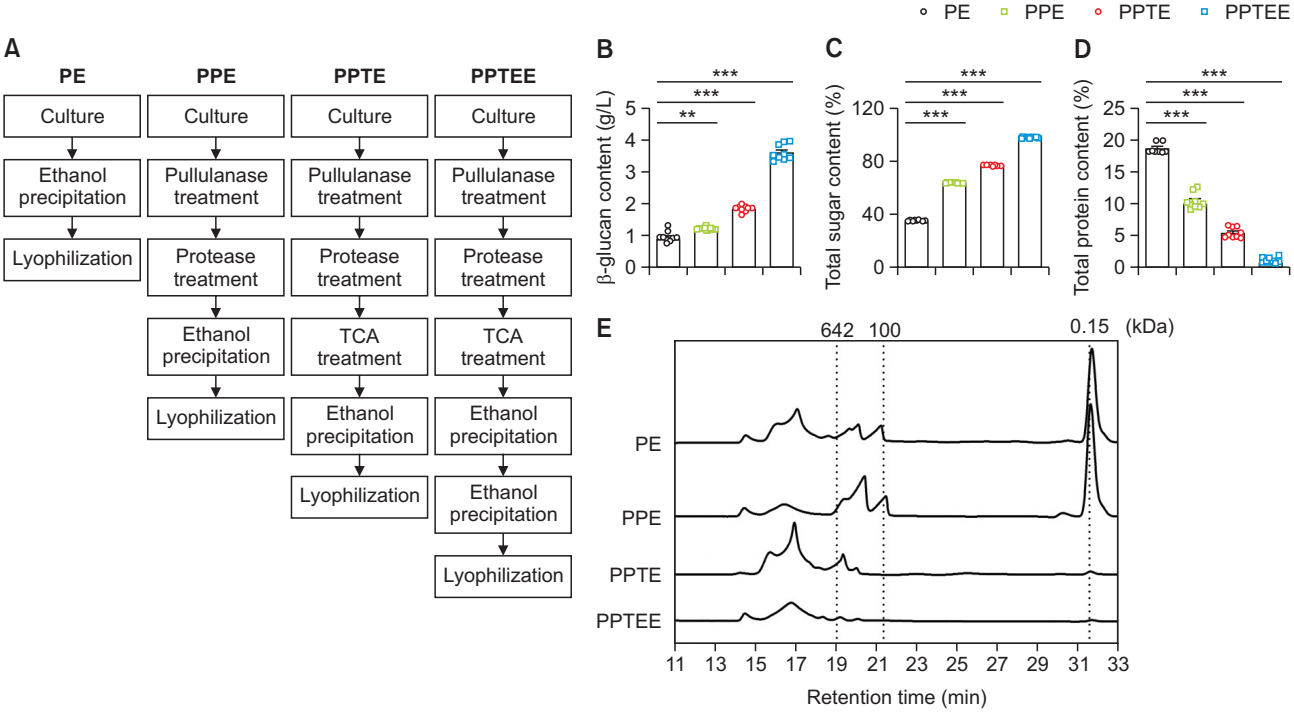

Fig. 1. PPTEE-glucan purification and physicochemical characteristics analysis. Purification processing diagram (A); β-glucan content (B); total sugar content (C); total protein content (D); molecular weight distribution (E). Statistical analysis was conducted using one-way ANOVA, with significance indicated as: $^{**}p<0.01$, $^{***}p<0.001$.

purification conditions, most of which were identified as glucose (Fig. 1E). Moreover, as the purification process progressed, most substances with molecular weights below 632 kDa were removed. This implied the elimination of substances other than β-glucan during the purification process, suggesting that the molecular weight distribution in the PPTEE condition is indicative of β-glucan.

Enhanced co-stimulatory molecule expression, pro-inflammatory cytokine production, and CD8⁺T cell activation in BMDCs treated with PPTEE-glucan

To verify the immunogenicity of PPTEE, we stimulated BMDC with OVA for 24 h in the presence of PPTEE and QS-21 as positive controls. The mean fluorescence intensity (MFI) of CD80, CD86, CD40, H2-K^b, and I-A/I-E in PPTEE-treated BMDC was significantly increased compared to that in the other groups (Fig. 2A-2F). However, co-treating with ME and PPTEE to BMDC couldn't enhance immune activation of PPTEE (Supplementary Fig. 1). Supernatants were collected from the stimulated BMDC to analyze pro-inflammatory cytokines levels. TNF-α, IL-1β, IL-6, and IL-12p40 were remarkably expressed in PPTEE-treated BMDC compared to OVA and OVA with QS-21 groups (Fig. 2G-2J). To assess the PPTEE-induced enhancement of antigen cross-presentation in BMDC, we co-cultured PPTEE-stimulated and OVA-treated BMDC with CellTrace Violet-stained OT-I CD8⁺T cells. PPTEE-treated BMDC showed significantly increased OT-I CD8⁺T cell proliferation at both ratios compared to that of BMDC treated with OVA alone, though not in QS-21-stimulated and OVA-treated BMDC (Fig. 2K). These data indicate that PPTEE can stimulate BMDCs into an immunogenic state, enhancing the expression of co-stimulatory markers, inflammatory cytokine production, and CD8⁺ T cell proliferation, ultimately increasing soluble antigen cross-presentation. These findings indicate the potential of PPTEE-glucan as an immune adjuvant that activates antigen-presenting cells.

PPTEE-glucan-containing ME increased antigen-specific immune responses

We developed a ME system containing PPTEE-glucan (ME+PPTEE) and assessed its potential as a vaccine adjuvant. We confirmed OVA+ME contains comparable amount of OVA compared to the OVA control (Supplementary Fig. 2). The particle properties of the ME+PPTEE and OVA+ME+PPTEE formulations were investigated (Supplementary Fig. 3). The hydrodynamic size of the ME+PPTEE group was 318.1 ± 56.33 nm, whereas that of the OVA+ME+PPTEE group was 410.37 ± 44.28 nm. Additionally, the zeta potential value of the ME+PPTEE group was 2.66 ± 0.11 mV, while that of the OVA+ME+PPTEE group was 11.90 ± 0.63 mV. The spherical shapes and comparable diameters (to hydrodynamic diameters in Supplementary Fig. 3) of ME+PPTEE and OVA+ME+PPTEE were observed in TEM image (Supplementary Fig. 4). The average content of PPTEE in ME, analyzed by HPLC system, was 63.22%. Mice were intramuscularly injected with OVA-containing ME or ME+PPTEE. PPTEE alone treatment failed to induce vaccination (Supplementary Fig. 5). Both ME-and ME+PPTEE-treated groups exhibited higher titers of IgG1, IgG2b, and IgG2c compared to the OVA control group. Notably, the IgG2b titer was significantly higher in the serum of ME+PPTEE-treated mice (Fig. 3A-3D). The higher IgG2b(Area Under Curve, AUC)/IgG1(AUC) ratio observed in ME+PPTEE-treated mice compared to that in ME-treated mice suggested the induction of a Th1 immune response in C57BL/6 mice (Fig. 3E). To evaluate antigen-specific T cell responses in vaccinated mice, splenocytes were stimulated with OVA. While IFN-γ expression in CD4+T cells was comparable among all groups, CD8⁺T cells from ME+PPTEE-treated mice showed significantly increased IFN-γ expression compared to that of the ME-treated group (Fig. 3F). To confirm the immunogenicity of PPTEE *in vivo*, OT-I CD8⁺T cells were injected into naïve mice, and their proliferation was observed. Mice that were subcutaneously administered PBS, OVA+ME, OVA+QS21, or OVA+ME+PPTEE were examined. OT-I CD8⁺T cells in ME+PPTEE-treated mice exhibited greater proliferation than that in ME-treated mice, comparable to that of QS-21 (Fig. 3G). These data demonstrate that PPTEE is a promising vaccine adjuvant that enhances antigen-specific immune responses.

PPTEE-glucan treatment mitigated cancer growth in tumor-bearing mice

Building on the observed activation of BMDCs and enhanced antigen-specific immune responses following PPTEE treatment, we evaluated the potential of PPTEE in mitigating cancer growth using a murine tumor model. Intratumoral injections of ME formulations, including ME alone, QS-21-containing ME (ME+QS-21), and PPTEE-containing ME (ME+PPTEE), were administered to MC38-bearing mice. Although ME alone failed to induce anti-cancer effects, the mice treated with ME+QS-21 and ME+PPTEE exhibited reduced cancer growth and tumor mass (Fig. 4A, 4B). Studies have reported that β-glucan treatment in cancer-bearing mice can reduce cancer growth by modulating MDSCs to become immunogenic (Albeituni *et al*., 2016). In the tumors of ME+PPTEE-treated mice, an increased infiltration of monocytic-MDSC (M-MDSC)-like cells expressing CD11b and Ly6C was observed, compared to that in the PBS- or ME-treated groups. In contrast, no significant change was observed in CD11b and Ly6G (Fig. 4C). Additionally, we noted a higher number of apoptotic cells in the tumor tissues of mice treated with ME+QS-21 and ME+PPTEE, which correlated with a reduction in tumor volume and mass (Fig. 4D). To explore whether PPTEE-glucan can induce the differentiation of M-MDSCs into immunogenic cells, we examined phenotypic changes in CD11b⁺LyC6⁺ cells in the presence of PPTEE. During BM-MDSC differentiation using IL-6 and GM-CSF, QS-21 or PPTEE was introduced. Both QS-21 and PPTEE increased the expression of Ly6C in differentiated cells, with QS-21 inducing more CD11b⁺Ly6C⁺ cells than PPTEE (Fig. 5A). Furthermore, while assessing the expression level of F4/80 in CD11b⁺Ly6C⁺ cells, PPTEE induced a higher level of F4/80 expression than QS-21 (Fig. 5B). This suggests that PPTEE leads to the generation of more immunogenic F4/80⁺CD11b⁺Ly6C⁺ cells than MDSCs. Investigating the characteristics of those M-MDSC-like cells differentiated in the presence of QS-21 and PPTEE, we conducted an assessment of cytokine production, including IL-1β, TNF-α, and IL-12p40 (Fig. 5C-5E). QS-21 treatment notably increased IL-1β secretion, while PPTEE treatment exhibited IL-1β secretion comparable to vehicle-treated MDSCs. Conversely, the secretion of TNF-α and IL-12p40 was significantly enhanced in the PPTEE-treated group compared to those in both QS-21-treated CD11b⁺Ly6C⁺ cells and vehicle-treated MDSCs. These findings collectively suggest the potential of PPTEE-

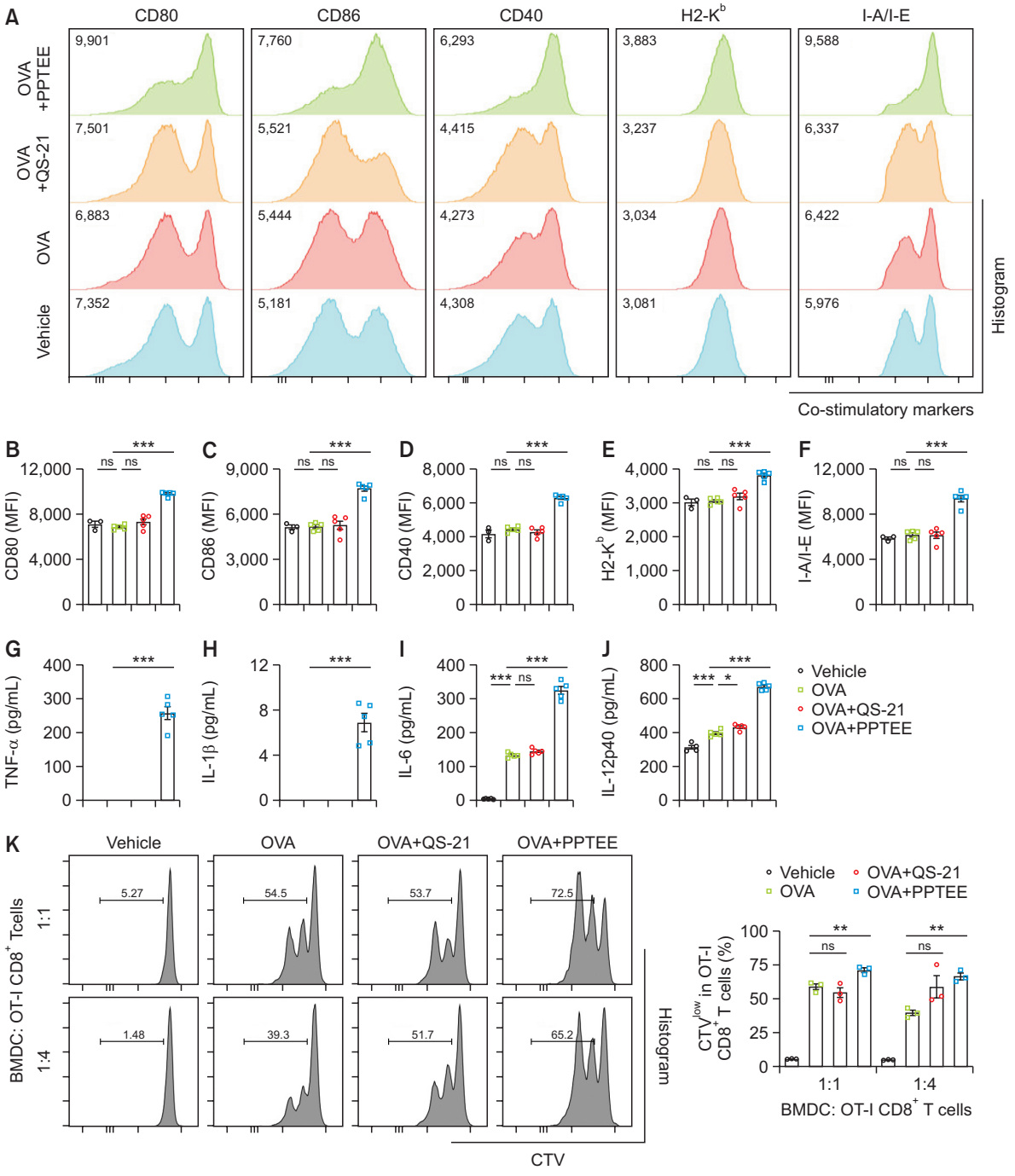

Fig. 2. Activation of BMDC by PPTEE-glucan for enhanced immune response. The BMDCs were stimulated with OVA alone, OVA+QS-21, or OVA+PPTEE for 24 h. Representative histograms of co-stimulatory markers (CD80, CD86, CD40, H2-K^b, and I-A/I-E) on BMDCs were analyzed by flow cytometry (A). Expression of CD80 (B), CD86 (C), CD40 (D), H2-K^b (E), and I-A/I-E (F) in BMDC. Supernatant from the cultured medium of stimulated BMDCs was collected, and pro-inflammatory cytokines TNF-α (G), IL-1β (H), IL-6 (I), and IL-12p40 (J) were measured using ELISA. Stimulated BMDCs were co-cultured with CellTrace Violet (CTV)-stained OT-I CD8$^+$T cells at the indicated ratios for 2 days. The proliferation of OT-I CD8$^+$T cells was analyzed using flow cytometry (K). The data is presented as mean ± SEM. Statistical analysis was conducted using a one-way ANOVA, with significance: non-significant (ns) when p≥0.05, **p*<0.05, ***p*<0.01, and ****p*<0.001.

glycan, a highly purified soluble β-1,3/1,6-glucan derived from *Aureobasidium pullulans*, in inducing anti-cancer effects, potentially through the augmentation of immunostimulatory activity of MDSCs.

DISCUSSION

Our findings demonstrated enhanced expression of co-stimulatory markers, pro-inflammatory cytokines, and cross-

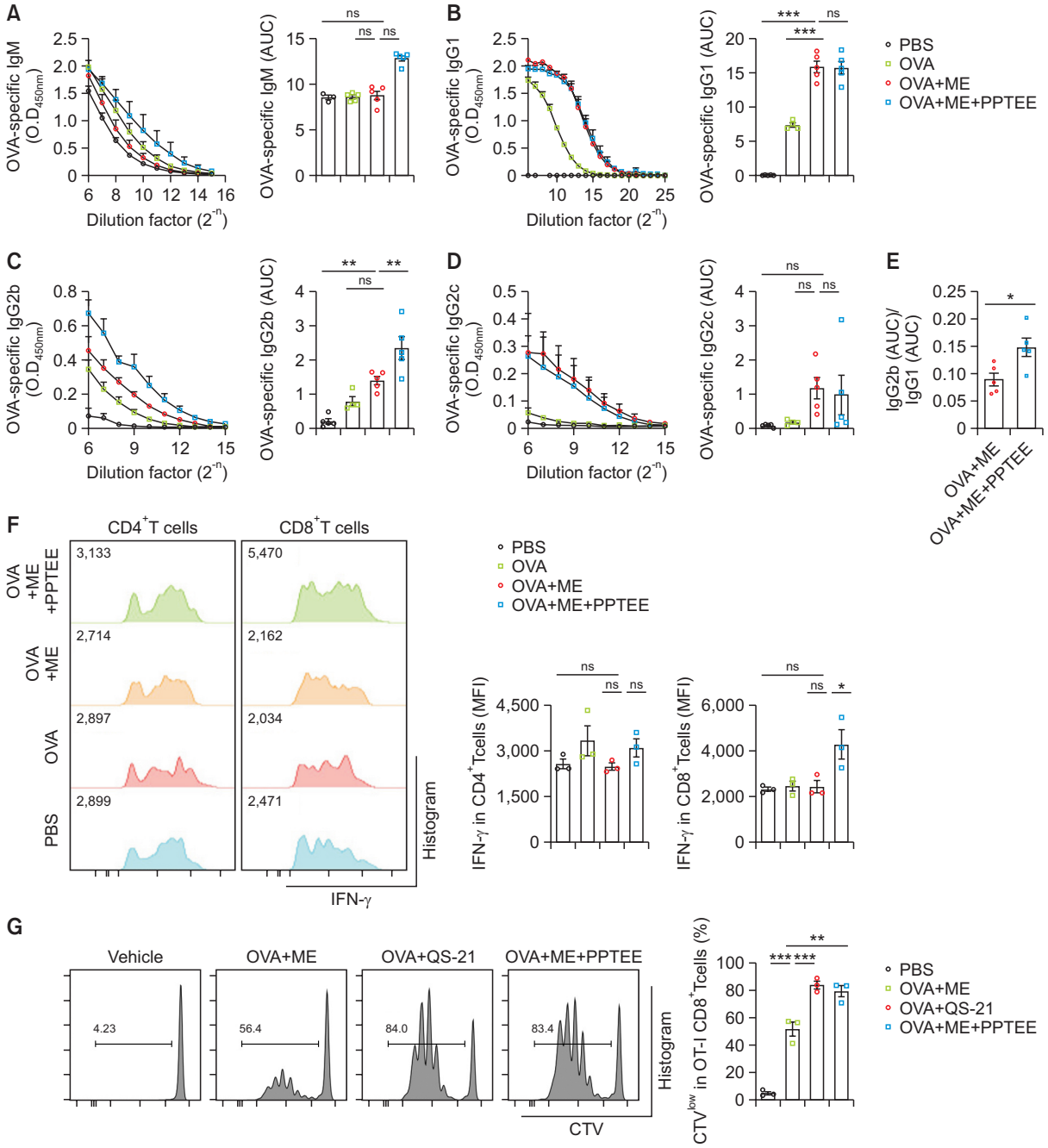

Fig. 3. Promotion of antigen-specific immune responses by PPTEE-glucan in C57BL/6 mice. C57BL/6 mice were vaccinated with OVA-containing microemulsion (ME) every 2 weeks for a total of 3 vaccinations. Serum was collected 21 days post-vaccine injection, and the titer and Area Under Curve (AUC) of OVA-specific IgM (A), IgG1 (B), IgG2b (C), and IgG2c (D) in the serum were analyzed by ELISA. (E) The AUC ratio of OVA-specific IgG1 to OVA-specific IgG2b was calculated (E). At 35 d post-vaccine injection, the spleens of vaccinated mice were extracted, and splenocytes were stimulated with an OVA-containing growth medium for 3 days. IFN-γ-expressing CD4+T cells and $CD8^+$T cells were analyzed using flow cytometry (F). For the *in vivo* $CD8^+$T cell proliferation assay, C57BL/6 recipient mice were injected with QS-21- and PPTEE-containing ME the day after transferring CD45.1 OT-I $CD8^+$T cells. Three days after ME injection, CD45.1 OT-I $CD8^+$T cells in the spleen were analyzed by flow cytometry (G). The data is presented as mean ± SEM. Statistical analysis was conducted using the unpaired t-test for (E) and one-way ANOVA for (A-D, F, G), with significance: non-significant (ns) when $p \geq 0.05$, *$p<0.05$, **$p<0.01$, ***$p<0.001$.

presentation abilities in PPTEE-treated BMDCs *in vitro*. *In vivo* experiments using a PPTEE+ME containing OVA showed elevated levels of antibodies, particularly IgG2b, in PPTEE-treated mice. Further analysis revealed increased IFN-γ expression in $CD8^+$T cells from splenocytes of PPTEE-treated mice stimulated with OVA, accompanied by induction of OT-I

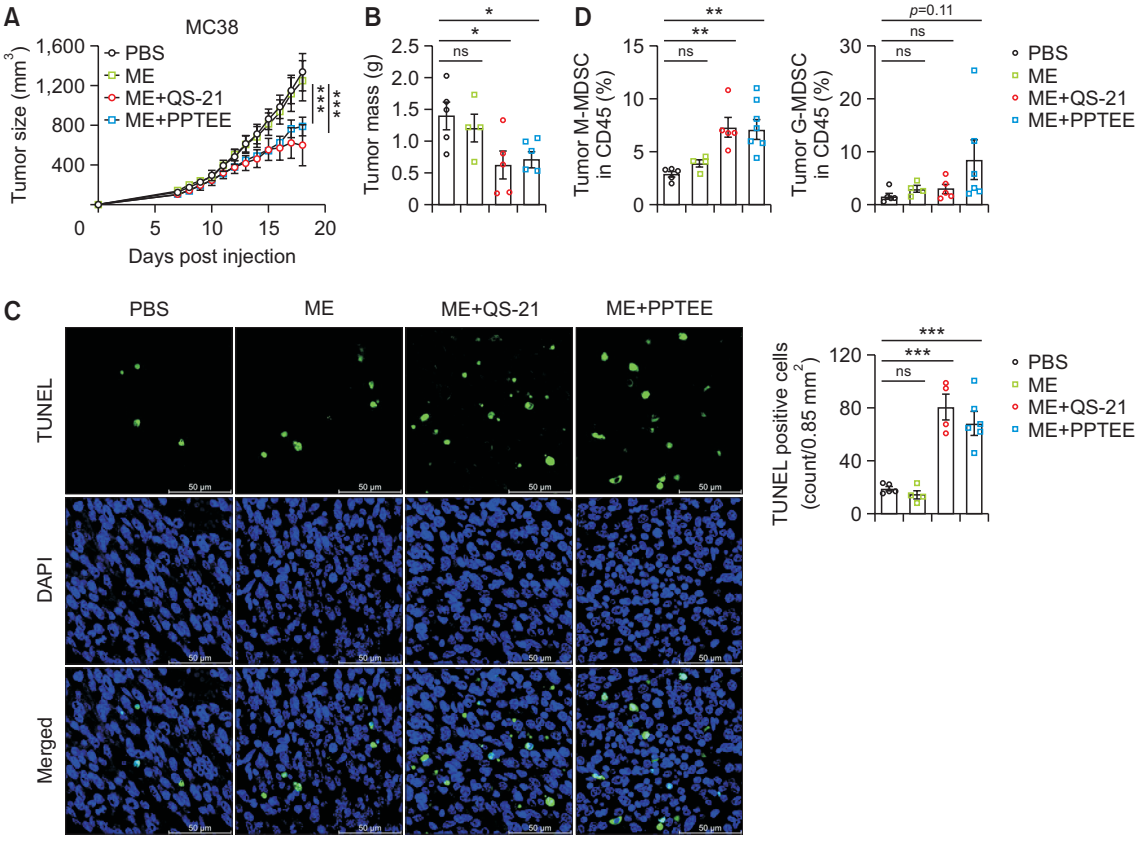

Fig. 4. Mitigation of tumor growth by intratumor injection of PPTEE-containing microemulsion (ME). QS-21- or PPTEE-containing ME was injected every 3 days into MC38-bearing C57BL/6 mice, starting 7 days after tumor inoculation. Tumor size (A) and mass (B) were measured until the mice were sacrificed. A TUNEL assay was performed on tumor tissues from each group of tumor-bearing mice. Representative sections of tumor tissue slides were shown (×400, scale bar: 50 μm) (C). Tumor-infiltrating myeloid-derived suppressive cells were analyzed by flow cytometry (D). The data is presented as mean ± SEM. Statistical analysis was conducted using two-way ANOVA for (A) and one-way ANOVA for (B-D), with significance: non-significant (ns) when $p \geq 0.05$, *$p<0.05$, **$p<0.01$, ***$p<0.001$.

$CD8^+$T cell proliferation. Intratumoral administration of ME-PPTEE to MC38-bearing mice resulted in notable amelioration of cancer growth associated with the generation of immunogenic MDSC.

MDSCs of the myeloid lineage share specific characteristics with monocytes and neutrophils and their immunosuppressive function contributes to the pathogenesis of cancer by inhibiting anti-cancer T cells, promoting regulatory T cell differentiation, supporting angiogenesis, and creating a metastatic environment (Umansky *et al*., 2016; Veglia *et al*., 2021). Depletion of MDSCs, inhibition of their recruitment, and activation of the immune system can elucidate their pathogenic roles (Veglia *et al*., 2021). In our study, MDSCs differentiated into immunostimulatory antigen-presenting cells, resulting in improved antigen-specific Th1 and $CD8^+$T cell activation. Recent studies also indicate that β-glucan-mediated reprogramming of MDSCs leads to the acquisition of a trained immunity phenotype, ultimately inducing anti-cancer immunity (Albeituni *et al*., 2016; Ding *et al*., 2023). Notably, yeast-derived β-glucan plays a crucial role in cancer regression by inducing apoptosis in MDSCs, promoting their differentiation into antigen-presenting cells, and enhancing the anti-tumor immune response by overcoming MDSC immunosuppression (Hong *et al*., 2004). Collectively, these findings suggest the potential use of β-glucan as a therapeutic strategy for enhancing immune responses against cancer.

Our data demonstrate an increased $CD11b^+Ly6C^+$ cell population in tumors of PPTEE-glucan-treated mice, as well as *in vitro*-differentiated BM-derived $CD11b^+Ly6C^+$ cells in the presence of PPTEE, with increased F4/80 expression and TNF-α secretion. This highlights the potential of soluble β-1,3/1,6-glucan generated by *Aureobasidium pullulans* to induce trained immunity, thereby activating myeloid cell functions. Moreover, β-glucan's influence on Th1 differentiation through the β-1,3 structure (Lee *et al*., 2021) aligns with our observations of increased $CD11b^+Ly6C^+$ cells and antigen-specific $CD8^+$T cell activation. This suggests that PPTEE-glucan induces immune activation in both myeloid and lymphoid cells. Collectively, these features can be strategically utilized in the development of soluble β-glucan-containing anti-cancer drugs.

The immunologic activity and binding to its receptors, CR3 and dectin-1, of β-glucan are determined by variable molecular characteristics such as the degree of polymerization, branches, length, and solubility, depending on its sources (Han *et al*., 2020). The high molecular weight of β-glucan stimulates phagocytes, increasing phagocytosis, cytotoxicity, and microbicidal activity. Conversely, low molecular weights are known

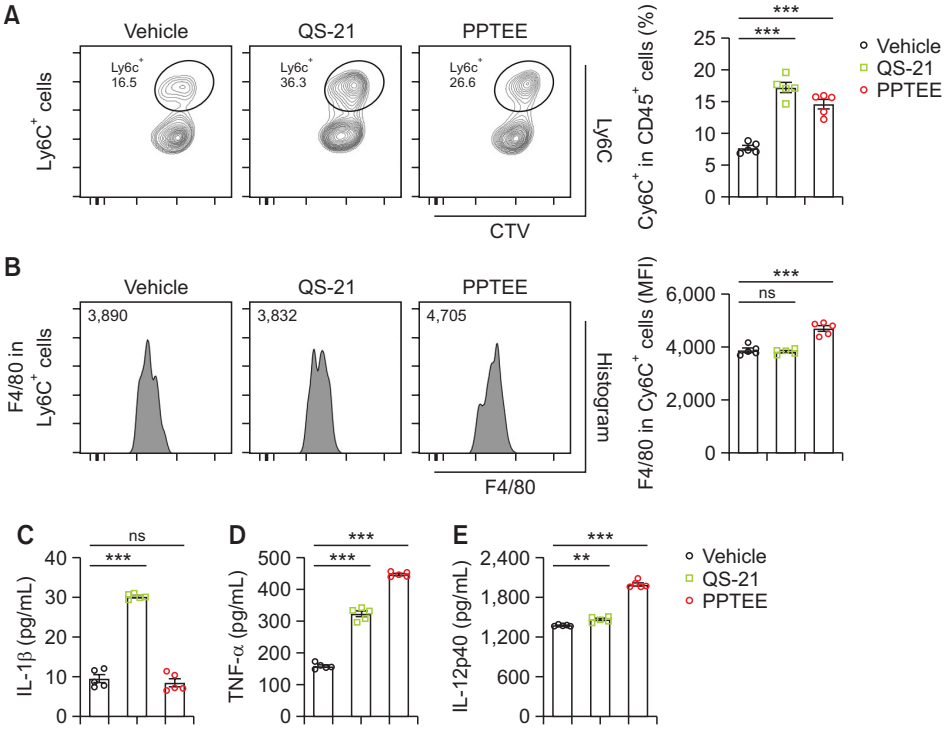

Fig. 5. Enhancement of immune activity in myeloid-derived suppressive cells by PPTEE-glucan. Differentiated MDSCs were stimulated with QS-21 or PPTEE for 24 h, respectively. The percentage of Ly6C-positive cells (A) and the Mean Fluorescence Intensity (MFI) of F4/80 in CD11b$^+$Ly6C$^+$ cells (B) were analyzed using flow cytometry. Pro-inflammatory cytokines, including IL-1β (C), TNF-α (D), and IL-12p40 (E), in the supernatant from MDSCs cultured with each adjuvant were measured using ELISA. Statistical analysis was conducted using a one-way ANOVA, with significance: non-significant (ns) when $p \geq 0.05$, $^{**}p<0.01$, and $^{***}p<0.001$.

to stimulate less (Adachi *et al*., 1990; Brown and Gordon, 2003; Lei *et al*., 2015). However, the increasing viscosity of β-glucan as a higher molecular weight remains a limitation for utilizing it as an adjuvant (Kim and White, 2013). To overcome this limitation, in the current study, we used β-glucan with high purity derived from *Aureobasidium pullulans*, which is well known to generate β-1,3/1,6-glucan (Suzuki *et al*., 2021). Our data demonstrated BDMC stimulation of *in vitro* and *in vivo* vaccination efficacy with antibody production. In this context, we proved that high-purity β-glucan generated by *Aureobasidium pullulans* can stimulate immune cells to induce adaptive immune responses, suggesting that the high purity of β-glucan promotes sufficient immune cell stimulation. These results indicate that PPTEE-glucan can be utilized in the medical and vaccine industries.

β-glucan has demonstrated its potential as a vaccine adjuvant. In the context of hepatitis B vaccination, curdlan, a β-glucan derived from the cell wall of *Alcaligenes faecalis*, demonstrated enhanced immunogenicity in mice compared to Alum during hepatitis B infection (Li *et al*., 2014). The use of β-glucan also increased resistance to influenza infection, strengthening the activity of neutrophils and NK cells (Vetvicka and Vetvickova, 2015). Furthermore, oral immunization with β-glucan-encapsulated OVA resulted in heightened intestinal IgA production, along with increased IFN-γ and IL-17A production in CD4$^+$T cells (De Smet *et al*., 2013). Mucosal immunization with curdlan prevents enteroviral infection and is associated with increased Th17 responses and IgA secretion (Yi *et al*., 2023). While oral-route vaccination with β-glucan showed abundant IgA secretion in mucosal regions, other injection routes, such as subcutaneous or intraperitoneal administration of β-glucan, induced IgG or IFN-γ-dependent disease amelioration rather than IgA (Huang *et al*., 2010; Lee *et al*., 2021). Our findings indicated improved anticancer effects and antigen-specific IgG secretion following antigen immunization with PPTEE-containing ME. In the context of vaccine adjuvants, β-glucan holds promise for its potential to enhance immunogenicity and mucosal barriers, mainly when administered through oral or mucosal routes.

Cancer is characterized by the establishment of a TME that suppresses anti-cancer immune responses (Shimizu *et al*., 2018; Wagner *et al*., 2020; Lao *et al*., 2022). To overcome this immunosuppressive nature, several agonists targeting pattern recognition receptors such as TLR or STING have been employed to activate antigen-presenting cells, thereby increasing antigen cross-presentation and the expression of pro-inflammatory cytokines (Alloatti *et al*., 2015; Fu *et al*., 2015; Luchner *et al*., 2021). In this regard, the interaction of β-glucan with dectin-1 on dendritic cells initiates the Syk/CARD9 pathway and leads to the secretion of IL-1β, IL-12, and IL-23. This, in turn, induces Th1/Th17 differentiation (Drummond and Brown, 2011; Saijo and Iwakura, 2011). However, Th17 cells can promote a pro-cancer environment by inducing angiogenesis and tumor growth (Marques *et al*., 2021). Moreover, orally administered β-1,3-Glucan was found to enhance the tumoricidal activity of antitumor monoclonal antibodies in murine tumor models by priming immune cells, specifically granulocytes and macrophages, through CR3 activation. This activation led

to improved killing of tumor cells coated with iC3b, and this mechanism did not rely on T cells and NK cells, however, primarily involved granulocytes. Combination therapy is promising for enhancing the efficacy of cancer treatment through a distinct immunomodulatory approach (Hong *et al*., 2004). We also observed the potential of β-glucan as an immune stimulator, inducing dendritic cell activation and antigen-specific cytotoxic T cell activity, such as IFN-γ-expressing $CD8^+$T cells. Furthermore, ME+PPTEE inhibited MC38 tumor growth. These results suggest that β-glucan induces Th1 responses rather than Th17 in our cancer mouse model.

In the late 1990s, the emulsion adjuvant MF59 was licensed and showed the potential to prevent pandemic influenza by enhancing cytotoxic immune activity (Khurana *et al*., 2010). The continuous development of insoluble adjuvants such as AS01, AS03, and AS04 has enabled vaccination against diseases that were previously challenging to immunize (Pulendran *et al*., 2021). Understanding the innate immune system has paved the way for enhancing current vaccines by activating TLRs on dendritic cells using PAMPs, thereby strengthening T cell and B cell responses (Kawai and Akira, 2010). Despite progress in adjuvants, only a limited number have received licensing owing to various issues, including tolerance, excessive inflammation, and safety concerns. Consequently, the development of innovative adjuvants capable of overcoming these constraints while ensuring a high level of immune stimulation, covering both humoral and cellular immunity, is emphasized. We used ready-to-use ME blended with an antigen prior to injection, which is practical and efficient for inducing local vaccination (Lee *et al*., 2016). ME system composed of Labrasol, Tween 80, mineral oil, and DW was developed based on the pseudo-ternay phase diagram (Lee *et al*., 2016). This ME offers advantages, such as ease of production, simple materials, and effective immune activation. ME+PPTEE formulation was designed through simple mixing of the oil phase (based on Labrasol, Tween 80, and mineral oil) and the water phase (including PPTEE) and its particle properties were confirmed by using TEM. The treatment with β-glucan has the potential to induce mucosal protection, anti-cancer activity, and microbicidal effects (De Smet *et al*., 2013; Lee *et al*., 2021; Yi *et al*., 2023). However, since mineral oil has disadvantage for inducing granuloma, it is required to using alternative gradients such as vegetable oil or highly refined of mineral oil to adjust on clinical trial (Pirow *et al*., 2019). Combining the efficiency of ME and PPTEE-glucan, along with the versatile advantages and safety of the host inherent in these natural products, could provide a valuable approach to enhancing public health against pathogens or pandemics, particularly in developing or least-developed countries.

In summary, we confirmed the potential of highly purified soluble PPTEE-glucan generated by *Aureobasidium pullulans* to improve antigen-specific immune responses and dendritic cell activation. Additionally, PPTEE-glucan demonstrated efficacy as an immune adjuvant in preventing cancer progression, particularly with respect to the polarization of immunogenic M-MDSCs into immunogenic myeloid cells.

REFERENCES

Adachi, Y., Ohno, N., Ohsawa, M., Oikawa, S. and Yadomae, T. (1990) Change of biological activities of (1----3)-beta-D-glucan from Grifola frondosa upon molecular weight reduction by heat treatment. *Chem. Pharm. Bull. (Tokyo)* **38**, 477-481.

Albeituni, S. H., Ding, C., Liu, M., Hu, X., Luo, F., Kloecker, G., Bousamra, M., 2nd, Zhang, H. G. and Yan, J. (2016) Correction: yeast-derived particulate beta-glucan treatment subverts the suppression of myeloid-derived suppressor cells (mdsc) by inducing polymorphonuclear MDSC apoptosis and monocytic MDSC differentiation to APC in cancer. *J. Immunol.* **196**, 3967.

Alloatti, A., Kotsias, F., Pauwels, A. M., Carpier, J. M., Jouve, M., Timmerman, E., Pace, L., Vargas, P., Maurin, M., Gehrmann, U., Joannas, L., Vivar, O. I., Lennon-Dumenil, A. M., Savina, A., Gevaert, K., Beyaert, R., Hoffmann, E. and Amigorena, S. (2015) Toll-like receptor 4 engagement on dendritic cells restrains phago-lysosome fusion and promotes cross-presentation of antigens. *Immunity* **43**, 1087-1100.

Baghban, R., Roshangar, L., Jahanban-Esfahlan, R., Seidi, K., Ebrahimi-Kalan, A., Jaymand, M., Kolahian, S., Javaheri, T. and Zare, P. (2020) Tumor microenvironment complexity and therapeutic implications at a glance. *Cell Commun. Signal.* **18**, 59.

Bayat Mokhtari, R., Homayouni, T. S., Baluch, N., Morgatskaya, E., Kumar, S., Das, B. and Yeger, H. (2017) Combination therapy in combating cancer. *Oncotarget* **8**, 38022-38043.

Berraondo, P., Sanmamed, M. F., Ochoa, M. C., Etxeberria, I., Aznar, M. A., Perez-Gracia, J. L., Rodriguez-Ruiz, M. E., Ponz-Sarvise, M., Castanon, E. and Melero, I. (2019) Cytokines in clinical cancer immunotherapy. *Br. J. Cancer* **120**, 6-15.

Brown, G. D. and Gordon, S. (2003) Fungal beta-glucans and mammalian immunity. *Immunity* **19**, 311-315.

Camilli, G., Tabouret, G. and Quintin, J. (2018) The complexity of fungal beta-glucan in health and disease: effects on the mononuclear phagocyte system. *Front. Immunol.* **9**, 673.

De Smet, R., Demoor, T., Verschuere, S., Dullaers, M., Ostroff, G. R., Leclercq, G., Allais, L., Pilette, C., Dierendonck, M., De Geest, B. G. and Cuvelier, C. A. (2013) beta-Glucan microparticles are good candidates for mucosal antigen delivery in oral vaccination. *J. Control. Release* **172**, 671-678.

Ding, C., Shrestha, R., Zhu, X., Geller, A. E., Wu, S., Woeste, M. R., Li, W., Wang, H., Yuan, F., Xu, R., Chariker, J. H., Hu, X., Li, H., Tieri, D., Zhang, H. G., Rouchka, E. C., Mitchell, R., Siskind, L. J., Zhang, X., Xu, X. G., McMasters, K. M., Yu, Y. and Yan, J. (2023) Inducing trained immunity in pro-metastatic macrophages to control tumor metastasis. *Nat. Immunol.* **24**, 239-254.

Drummond, R. A. and Brown, G. D. (2011) The role of Dectin-1 in the host defence against fungal infections. *Curr. Opin. Microbiol.* **14**, 392-399.

DuBois, M., Gilles, K. A., Hamilton, J. K., Rebers, P. A. and Smith, F. (1956) Colorimetric method for determination of sugars and related substances. *Anal. Chem.* **28**, 350-356.

Fu, J., Kanne, D. B., Leong, M., Glickman, L. H., McWhirter, S. M., Lemmens, E., Mechette, K., Leong, J. J., Lauer, P., Liu, W., Sivick, K. E., Zeng, Q., Soares, K. C., Zheng, L., Portnoy, D. A., Woodward, J. J., Pardoll, D. M., Dubensky, T. W., Jr. and Kim, Y. (2015) STING agonist formulated cancer vaccines can cure established tumors resistant to PD-1 blockade. *Sci. Transl. Med.* **7**, 283ra252.

Goodridge, H. S., Wolf, A. J. and Underhill, D. M. (2009) Beta-glucan recognition by the innate immune system. *Immunol. Rev.* **230**, 38-50.

Han, B., Baruah, K., Cox, E., Vanrompay, D. and Bossier, P. (2020) Structure-functional activity relationship of beta-glucans from the perspective of immunomodulation: a mini-review. *Front. Immunol.* **11**, 658.

Hong, F., Yan, J., Baran, J. T., Allendorf, D. J., Hansen, R. D., Ostroff, G. R., Xing, P. X., Cheung, N. K. and Ross, G. D. (2004) Mechanism by which orally administered beta-1,3-glucans enhance the tumoricidal activity of antitumor monoclonal antibodies in murine tumor models. *J. Immunol.* **173**, 797-806.

Huang, H., Ostroff, G. R., Lee, C. K., Specht, C. A. and Levitz, S. M. (2010) Robust stimulation of humoral and cellular immune responses following vaccination with antigen-loaded beta-glucan particles. *mBio* **1**, e00164-10.

Huang, L., Xu, H. and Peng, G. (2018) TLR-mediated metabolic reprogramming in the tumor microenvironment: potential novel strate-

gies for cancer immunotherapy. *Cell. Mol. Immunol.* **15**, 428-437.
Ikewaki, N., Dedeepiya, V. D., Raghavan, K., Rao, K. S., Vaddi, S., Osawa, H., Kisaka, T., Kurosawa, G., Srinivasan, S., Kumar, S. R. B., Senthilkumar, R., Iwasaki, M., Preethy, S. and Abraham, S. J. K. (2022) beta-glucan vaccine adjuvant approach for cancer treatment through immune enhancement (B-VACCIEN) in specific immunocompromised populations (review). *Oncol. Rep.* **47**, 14.
Kawai, T. and Akira, S. (2010) The role of pattern-recognition receptors in innate immunity: update on Toll-like receptors. *Nat. Immunol.* **11**, 373-384.
Khurana, S., Chearwae, W., Castellino, F., Manischewitz, J., King, L. R., Honorkiewicz, A., Rock, M. T., Edwards, K. M., Del Giudice, G., Rappuoli, R. and Golding, H. (2010) Vaccines with MF59 adjuvant expand the antibody repertoire to target protective sites of pandemic avian H5N1 influenza virus. *Sci. Transl. Med.* **2**, 15ra15.
Kim, H. J. and White, P. J. (2013) Impact of the molecular weight, viscosity, and solubility of beta-glucan on *in vitro* oat starch digestibility. *J. Agric. Food Chem.* **61**, 3270-3277.
Lao, Y., Shen, D., Zhang, W., He, R. and Jiang, M. (2022) Immune checkpoint inhibitors in cancer therapy-how to overcome drug resistance? *Cancers (Basel)* **14**, 3575.
Lee, C., Verma, R., Byun, S., Jeun, E. J., Kim, G. C., Lee, S., Kang, H. J., Kim, C. J., Sharma, G., Lahiri, A., Paul, S., Kim, K. S., Hwang, D. S., Iwakura, Y., Speciale, I., Molinaro, A., De Castro, C., Rudra, D. and Im, S. H. (2021) Structural specificities of cell surface beta-glucan polysaccharides determine commensal yeast mediated immuno-modulatory activities. *Nat. Commun.* **12**, 3611.
Lee, J. J., Shim, A., Lee, S. Y., Kwon, B. E., Kim, S. R., Ko, H. J. and Cho, H. J. (2016) Ready-to-use colloidal adjuvant systems for intranasal immunization. *J. Colloid Interface Sci.* **467**, 121-128.
Lei, N., Wang, M., Zhang, L., Xiao, S., Fei, C., Wang, X., Zhang, K., Zheng, W., Wang, C., Yang, R. and Xue, F. (2015) Effects of low molecular weight yeast beta-glucan on antioxidant and immunological activities in mice. *Int. J. Mol. Sci.* **16**, 21575-21590.
Li, P., Tan, H., Xu, D., Yin, F., Cheng, Y., Zhang, X., Liu, Y. and Wang, F. (2014) Effect and mechanisms of curdlan sulfate on inhibiting HBV infection and acting as an HB vaccine adjuvant. *Carbohydr. Polym.* **110**, 446-455.
Lin, M. J., Svensson-Arvelund, J., Lubitz, G. S., Marabelle, A., Melero, I., Brown, B. D. and Brody, J. D. (2022) Cancer vaccines: the next immunotherapy frontier. *Nat. Cancer* **3**, 911-926.
Luchner, M., Reinke, S. and Milicic, A. (2021) TLR agonists as vaccine adjuvants targeting cancer and infectious diseases. *Pharmaceutics* **13**, 142.
Marques, H. S., de Brito, B. B., da Silva, F. A. F., Santos, M. L. C., de Souza, J. C. B., Correia, T. M. L., Lopes, L. W., Neres, N. S. M., Dorea, R., Dantas, A. C. S., Morbeck, L. L. B., Lima, I. S., de Almeida, A. A., Dias, M. R. J. and de Melo, F. F. (2021) Relationship between Th17 immune response and cancer. *World J. Clin. Oncol.* **12**, 845-867.
Moorlag, S., Khan, N., Novakovic, B., Kaufmann, E., Jansen, T., van Crevel, R., Divangahi, M. and Netea, M. G. (2020) beta-Glucan induces protective trained immunity against mycobacterium tuberculosis infection: a key role for IL-1. *Cell Rep.* **31**, 107634.
Pirow, R., Blume, A., Hellwig, N., Herzler, M., Huhse, B., Hutzler, C., Pfaff, K., Thierse, H. J., Tralau, T., Vieth, B. and Luch, A. (2019) Mineral oil in food, cosmetic products, and in products regulated by other legislations. *Crit. Rev. Toxicol.* **49**, 742-789.
Pulendran, B., S Arunachalam, P. and O'Hagan, D. T. (2021) Emerging concepts in the science of vaccine adjuvants. *Nat. Rev. Drug Discov.* **20**, 454-475.
Reed, S. G., Orr, M. T. and Fox, C. B. (2013) Key roles of adjuvants in modern vaccines. *Nat. Med.* **19**, 1597-1608.
Saijo, S. and Iwakura, Y. (2011) Dectin-1 and Dectin-2 in innate immunity against fungi. *Int. Immunol.* **23**, 467-472.
Schirrmacher, V. (2019) From chemotherapy to biological therapy: a review of novel concepts to reduce the side effects of systemic cancer treatment (review). *Int. J. Oncol.* **54**, 407-419.
Schoenfeld, A. J. and Hellmann, M. D. (2020) Acquired resistance to immune checkpoint inhibitors. *Cancer Cell* **37**, 443-455.
Shimizu, K., Iyoda, T., Okada, M., Yamasaki, S. and Fujii, S. I. (2018) Immune suppression and reversal of the suppressive tumor microenvironment. *Int. Immunol.* **30**, 445-454.
Shui, Y., Hu, X., Hirano, H., Kusano, K., Tsukamoto, H., Li, M., Hasumi, K., Guo, W. Z. and Li, X. K. (2021) beta-Glucan from Aureobasidium pullulans augments the anti-tumor immune responses through activated tumor-associated dendritic cells. *Int. Immunopharmacol.* **101**, 108265.
Suzuki, T., Kusano, K., Kondo, N., Nishikawa, K., Kuge, T. and Ohno, N. (2021) Biological activity of high-purity beta-1,3-1,6-glucan derived from the black yeast aureobasidium pullulans: a literature review. *Nutrients* **13**, 242.
Tan, S., Li, D. and Zhu, X. (2020) Cancer immunotherapy: pros, cons and beyond. *Biomed. Pharmacother.* **124**, 109821.
Toor, S. M., Sasidharan Nair, V., Decock, J. and Elkord, E. (2020) Immune checkpoints in the tumor microenvironment. *Semin. Cancer Biol.* **65**, 1-12.
Umansky, V., Blattner, C., Gebhardt, C. and Utikal, J. (2016) The role of myeloid-derived suppressor cells (MDSC) in cancer progression. *Vaccines (Basel)* **4**, 36.
Veglia, F., Sanseviero, E. and Gabrilovich, D. I. (2021) Myeloid-derived suppressor cells in the era of increasing myeloid cell diversity. *Nat. Rev. Immunol.* **21**, 485-498.
Vetvicka, V. and Vetvickova, J. (2015) Glucan supplementation enhances the immune response against an influenza challenge in mice. *Ann. Transl. Med.* **3**, 22.
Wagner, J., Wickman, E., DeRenzo, C. and Gottschalk, S. (2020) CAR T cell therapy for solid tumors: bright future or dark reality? *Mol. Ther.* **28**, 2320-2339.
Yi, E. J., Kim, Y. I., Song, J. H., Ko, H. J. and Chang, S. Y. (2023) Intranasal immunization with curdlan induce Th17 responses and enhance protection against enterovirus 71. *Vaccine* **41**, 2243-2252.